Energy & Environmental Science

Cite this: *Energy Environ. Sci.*, 2012, **5**, 6973

www.rsc.org/ees

PAPER

Demonstration of high power, direct conversion of waste-derived carbon in a hybrid direct carbon fuel cell†

Cairong Jiang,[a] Jianjun Ma,[ab] Alfredo D. Bonaccorso[a] and John T. S. Irvine*[a]

Received 20th December 2011, Accepted 13th February 2012
DOI: 10.1039/c2ee03510c

Direct carbon fuel cells offer highly efficient means of converting carbon from waste, biomass or coal to electricity producing an exhaust stream that is well-suited to CO_2 sequestration and, hence could underpin a new, clean carbon economy. If this technology is to contribute significantly to improving our impending global energy crisis, three aspects must first be addressed: competitive performance with extant fuel cell technologies, development of practical systems to handle available carbon resources and demonstration of sufficient durability, *i.e.* 40 000 hours minimum for system. In the present study, we demonstrate excellent performance from a hybrid direct carbon fuel cell based upon an yttrium-stabilised zirconia electrolyte to use solid carbons as fuels directly. Good stability of the zirconia is observed during and after fuel cell testing and in corrosion tests under reducing conditions; however, significant intergrain erosion is observed under oxidising conditions. The carbon fuel chosen is a waste product, Medium Density Fibreboard, which is widely available and difficult to recycle. Cells exhibit excellent electrochemical performance at 750 °C, with a maximum power density of 390 mW cm^{-2} using a lanthanum doped strontium manganite (LSM) cathode and 878 mW cm^{-2} using a lanthanum doped strontium cobalt (LSC) cathode under flowing air. This is comparable with current commercial Solid Oxide Fuel Cell and significantly in excess of commercial Molten Carbonate Fuel Cell (MCFC) performance. This hybrid direct carbon fuel cell therefore offers the clean utilisation of coal, waste and renewable carbon sources and hence merits development as a realistic alternative technology.

Introduction

Carbon fuel cells are an emerging power generation technology that promise direct and efficient utilisation of abundant solid carbon reserves in the world. Carbon fuel cells allow the chemical energy in versatile feedstocks such as biomass (*e.g.* wood, coconut shell),[1] coal petroleum coke[2–4] (*e.g.* residue from the distillation unit in refinery plants), pyrolytic carbon (from natural gas),[5–8] and municipal carbon wastes[9] to be converted to electricity. The electrical efficiency of power generation from carbon fuel cells can theoretically reach up to ~100%, with practical efficiencies of around 80%. This compares to traditional coal or biomass-fired power plants, which are subject to thermodynamic limitation at ~40%.[10,11] In addition, carbon fuel cells offer the potential to produce less noise, lower pollution, and pure CO_2 without nitrogen diluent which could be available for sequestration, without expensive gas separation and energy intensive purification processes. The promise of carbon fuel cells arises not only from diversity of available fuels and high operating efficiency, but also a solid infrastructure for scale-up, including transportation, storage, and processing of fuels.

[a]*EaStCHEM, School of Chemistry, University of St Andrews, St Andrews, Fife, KY16 9ST, UK. E-mail: jtsi@st-andrews.ac.uk*
[b]*School of Materials Science and Engineering, Chonnam National University, Gwangju 500-757, Republic of Korea*

† Electronic supplementary information (ESI) available. See DOI: 10.1039/c2ee03510c

Broader context

Direct carbon fuel cells offer very high efficiency for converting carbon to electrical energy, potentially doubling conversion efficiency, with the added benefit of simpler and less energy wasteful sequestration of CO_2. As we globally expect to get perhaps 1/3 of our energy from coal and biomass carbons for the foreseeable future, this technology has created very significant interest worldwide, despite the fact that the technology is really at the proof of concept stage. In this study, we have achieved high performance levels taking direct carbon cells well beyond the threshold for exciting developmental interest for the first time. The two advances that have enabled this are applying very thin zirconia electrolytes and greatly reducing the carbonate to carbon ratio.

Solid carbon offers a large energy density (per unit volume), *i.e.* 20.0 kW h L^{-1}, compared to other fuels such as methane (4.2 kW h L^{-1}), hydrogen (2.4 kW h L^{-1}) and diesel (9.8 kW h L^{-1}).[12–14] Whilst coal remains an important source of carbon fuel, CO_2 emissions can be greatly decreased by the use of the high efficiency direct carbon fuel cell concept. However, renewable or "zero-carbon" carbon resources, *i.e.* biomass and pyrolytic waste materials (*e.g.* wood from forest clearance, paper, plastics), truly offer the potential for carbon neutral power generation. It is important to note that coal and biomass carbons contain significant and variable amounts of useful non-carbon species such as tars, and hence are not strictly carbon. As well as being of much more practical use, such impure carbons also tend to perform better in direct carbon fuel cells than pure carbons due to easier activation.

Jacques first reported a DCFC in 1896,[15,16] using a molten hydroxide electrolyte at 400–500 °C; however, there were problems with carbonate build up. Thereafter, unlike for hydrogen, there was not a sustained effort to develop carbon fuel cells. Interest was revived by Anbar and Weaver *et al.* in 1976[17] using carbonate as the electrolyte and proposing to use the CO_2 by-product of the carbon oxidation to keep the electrolyte stable. The cell consisted of a molten lead anode with the fuel-rich molten carbonate electrolyte (40% Li_2CO_3/30% K_2CO_3/30% Na_2CO_3) floating on top at an operating temperature of 650–750 °C. A similar idea utilising a liquid tin/tin oxide redox shuttle in a solid oxide fuel cell has been published by Tao *et al.*[18] and antimony/antimony oxide by Gorte *et al.*[19] The most significant advances for direct conversion of carbon have been achieved utilising MCFC-related technology following the lead of Cooper.[20,21] So far, the highest power density of 100 mW cm^{-2} has been obtained using highly disordered and activated carbon particulates in a MCFC type system by Cooper.[22] If the technology is to be considered for commercial scale up, this power level in single cells needs to be at least doubled.

Oxidation of solid carbon is generally viewed as very difficult in fuel cells. The intrinsic difficulty in implementing carbon fuels is that most fuel cells are based on a solid membrane;[23–26] this means that there is very little interaction between the solid fuel and the solid electrode. Therefore, most research to date has focused on high-temperature liquid electrolyte concepts. An alternative concept uses a hybrid molten carbonate/solid oxide electrode/electrolyte concept[27] with carbon mixed with the carbonate and either placed on top of a solid oxide[28,29] or with the solid electrolyte immersed in a slurry of liquid carbonate.[30,31] This liquid interface removes solid/solid contact problems and seems to provide a very attractive way forward. By employing a solid oxide electrolyte to separate the cathode and anode compartments, whilst utilising a molten carbonate electrolyte on the anode side it is possible to avoid the need for CO_2 circulation and to utilise well developed concepts for many of the fuel cell components. Alternative carbon fuel cell concepts to direct carbon oxidation have been also made to improve the sluggish solid reaction through fluidized bed,[23,32,33] stirred approach,[34,35] gasification into carbon monoxide before feeding to SOFC,[36,37] or indeed internal gasification using an iron catalyst.[38]

Here we showed a hybrid direct carbon fuel cell (HDCFC) using a solid oxide electrolyte to separate the cathode and anode compartments, while a molten carbonate electrolyte is utilised to extend the anode/electrolyte region (Fig. 1). Oxygen is reduced to O^{2-} ions at the cathode and transported across the solid electrolyte membrane to the anode compartment, where carbon is oxidised to CO_2.[39,40]

$$C + 2O^{2-} \rightarrow CO_2 + 4e^- \quad (1)$$

ΔG for this reaction is −395 kJ mol^{-1} and the ratio $\Delta G/\Delta H = 1.003$, meaning that this process theoretically offers 100% chemical to electrical conversion efficiency, more than twice as high as obtainable from thermal conversion. There are also alternative processes, for example, a partial oxidation of carbon to CO is also possible:

$$C + O^{2-} \rightarrow CO + 2e^- \quad (2)$$

These two reactions require solid/solid interaction as O^{2-} ions are supplied from the solid electrolyte; however, the fluidity of the molten carbonate would enhance the transport of the carbon fuel to the anode.[41,42] Whilst the carbonate eutectic melts at about 500 °C HDCFC performance does not increase greatly until near 700 °C where we believe the viscosity decreases and wetting ability increases significantly. Enhancement of the anode reaction by the molten carbonate as an electrochemical mediator is also expected:[22,43]

$$C + 2CO_3^{2-} \rightarrow 3CO_2 + 4e^- \quad (3)$$

$$C + CO_3^{2-} \rightarrow CO + CO_2 + 2e^- \quad (4)$$

These reactions should be followed by the regeneration of CO_3^{2-} ions in order that the electric charge of the molten carbonate can be kept neutral.

$$CO_2 + O^{2-} \rightarrow CO_3^{2-} \quad (5)$$

The carbon can be converted *via* a non-electrochemical reaction known as the reverse "Boudouard reaction", which increases in extent at higher temperatures:[44]

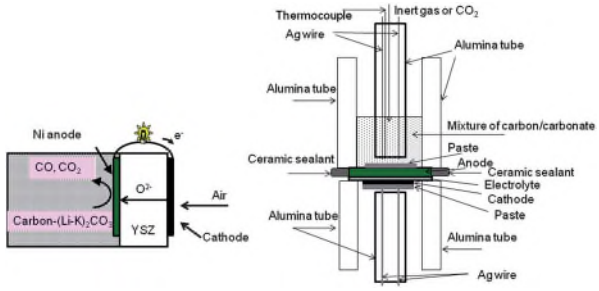

Fig. 1 Schematic of the hybrid direct carbon fuel cell, above left, and the used test geometry, right. The hybrid direct carbon fuel cell is the combination of a solid oxide fuel cell (SOFC) and a molten carbonate fuel cell; the SOFC is composed of a nickel based cermet, a YSZ electrolyte, and a $(La_{0.8}Sr_{0.2})_{0.95}MnO_{3-\delta}$/YSZ composite cathode or a $La_{0.6}Sr_{0.4}CoO_{3-\delta}$ (LSC) cathode; a mixture of carbon and lithium–potassium carbonate (62 mol% Li_2CO_3 : 38 mol% K_2CO_3) in a weight ratio of C : CO_3^{2-} = 4 : 1 is placed in the anode chamber, which is sealed to the SOFC; the reaction at the cathode is $O_2 + 4e^- = 2O^{2-}$ and the total reaction of the anode is that carbon is oxidised to CO_2.

$$C + CO_2 \rightarrow 2CO \quad (6)$$

The chemical energy of CO can still be converted to electric power *via* the electrochemical oxidation of CO at the anode in the DCFC:[37,45,46]

$$CO + O^{2-} \rightarrow CO_2 + 2e^- \quad (7)$$

In a small cell, it is also likely that produced CO_2 will react with un-oxidised carbon, removing it from the system as CO without complete oxidation. To avoid this process and maximise direct oxidation it is desirable to operate closer to 700 °C than 800 °C. In the more relevant fuels such as biomass-derived chars and coals, there are also electroactive species containing hydrogen, oxygen, nitrogen and perhaps sulfur that will be involved in the electrochemical process.

Experimental

Carbon processing and pre-treatment

The carbon fuel used in the direct carbon fuel cells (HDCFCs) is from Medium Density Fibreboard (MDF) made by pyrolysing at 400 °C in N_2 by Micro Power Energy (Glasgow, UK). A mixture of 62 mol% lithium carbonate (Aldrich Chemical Co., WI, USA) and 38 mol% potassium carbonate (Fisher, UK) was pre-mixed by ball milling in acetone for 24 h before being mixed with pyrolysed MDF (PMDF). The weight ratio of PMDF to Li_2CO_3–K_2CO_3 is 4 : 1. The same process was used for the PMDF–carbonate mixture, followed by drying in an oven at 80 °C overnight.

Electrolyte-supported cells preparation

Electrolyte-supported cells were obtained by screen printing a NiO (Aldrich, 325 mesh)-YSZ (Tosoh, TZ-8Y) (60/40) anode slurry and a $(La_{0.8}Sr_{0.2})_{0.95}MnO_{3-\delta}$ (PRAXAIR)–YSZ composite cathode slurry on each surface of the YSZ electrolyte, which was 1 mm thick and 20 mm in diameter and made by dry pressing and sintering at 1500 °C for 10 h. The anode was calcined at 1350 °C for 2 h and then the cathode was calcined at 1100 °C for 2 h. The area of the anode and the cathode was the same, which was 1.13 cm^2. The as-prepared cell was painted with silver paste (pre-treated at 800 °C for 1 h) on the anode and the cathode as the current collectors.

Anode-supported cells preparation

Anode-supported cells were prepared by slurry coating electrolyte onto an anode support. The anode substrate of nickel oxide (Sumitomo metal Mining Co. Ltd. Japan, 99.9%) and YSZ (Tosoh, TZ-8Y) with a 60 : 40 weight ratio was mixed by ball milling for 24 h and pressed into a disk with ~1 mm thickness. The slurry of YSZ was obtained by mixing YSZ powder with organic solutions, binders and plasticisers for 20 h. After that the YSZ slurry was coated onto the anode substrate. The half cell with the anode substrate and the thin YSZ electrolyte was sintered at 1350 °C for 5 h. The thickness of the YSZ electrolyte can be controlled by the slurry concentration, and in the present study, it was 5–10 μm. A cathode of either $(La_{0.8}Sr_{0.2})_{0.95}MnO_{3-\delta}$ (LSM)–YSZ or $La_{0.6}Sr_{0.4}CoO_{3-\delta}$ (LSC, PRAXAIR) was screen printed on the surface of the YSZ electrolyte, by calcining at 1100 °C and 900 °C, respectively. The cathode area of the anode-supported cell was the same as the cathode area of the electrolyte-supported cell. In order to avoid the reaction between the LSC cathode and the YSZ electrolyte, a layer of $Ce_{0.9}Gd_{0.1}O_{2-\delta}$ (PRAXAIR) (sintered at 1200 °C for 2 h) was screen printed on the surface of the YSZ thin membrane. Finally, the as-prepared cell with ~20 mm diameter was painted with silver paste, pre-calcined at 800 °C for 1 h, on both sides of the anode and the cathode. The anodes were painted with gold paste instead of silver paste for longer term tests.

Cell design and electrochemical characteristics

Either an electrolyte-supported cell or an anode-supported cell was sealed on the alumina tube using sealant (Aremco 552), with the anode side up. A 2 g mixture of PMDF–carbonate was weighed and filled into the anode chamber. The purge gas of N_2 or CO_2 was controlled by the valves and the flow rate of gas was 20 ml min^{-1} or ~7 ml min^{-1} in the longer term tests. The cell performance was measured on a Solartron 1280B with a 10 mV ac perturbation for AC impedance and 20 mV per step to scan current–voltage curves.

Cathode polarisation resistance measurement

The polarisation resistance of the LSM–YSZ composite cathode (50 wt% LSM) was tested on the symmetric cell of LSM–YSZ/YSZ/LSM–YSZ, with a pellet of YSZ obtained by dry pressing and sintering at 1500 °C for 10 h. The LSM–YSZ composite electrodes were calcined at 1100 °C for 2 h before the AC electrochemical impedance spectra measurement, which was carried out on a Solartron 1260 with a 50 mV ac perturbation. The pellet of $Ce_{0.9}Gd_{0.1}O_{2-\delta}$ was used for the LSC electrode polarisation resistance test. The calcination temperature for the LSC electrode was 900 °C, which was the same as the temperature for the LSC cathode of the anode-supported cell.

Etching samples in $(Li–K)_2CO_3$

8 mol% yttrium stabilised zirconia (TZ-8Y, Tosoh, Japan) powders were pressed into pellets and sintered at 1400 °C for 2 h. Pellets made from TZ-3Y and TZ-8Y were buried in lithium and potassium eutectic carbonate (62 mol% Li_2CO_3 : 38 mol% K_2CO_3) and heated up to 700 °C and dwelled for 10 h in air or argon or 5% H_2/Ar. The etched pellets were washed with dilute nitric acid (Aldrich, UK). The same etching process in air or argon or 5% H_2/Ar was applied to the cells after electrochemical measurement.

Gas chromatography analysis

The gas analysis was performed on an Agilent 3000 micro Gas Chromatograph equipped with two capillary columns and a back-flush injector. A 12 μm × 320 μm × 1 m MolSieve column equipped with a PlotU pre-column (30 μm × 320 μm × 3 m) with argon as the carrier gas was used for hydrogen, nitrogen, carbon monoxide and methane detection. A 30 μm × 320 μm × 8 m PlotU column equipped with a PlotQ pre-column (10 μm × 320 μm × 1 m) with

helium carrier gas was used for carbon dioxide detection. Injection occurred through a backflush injector operated at 130 °C. The separation occurred at 85 °C and 100 °C with a pressure of 32 psi and 30 psi for MolSieve column and Plot column, respectively. In longer term tests the percentages of gas output were determined, these were converted to gas volumes using the nitrogen purge gas as an internal standard and as this slightly overestimated the amount of carbon produced over long term tests, these were then normalised against the total amount of carbon utilised.

Other characterisations

The elements of carbon, hydrogen, nitrogen and sulfur in PMDF were analysed with CHNS element analysis (EA 1110 CHNS). The microstructures of the cross-section of the cells and the surface of the YSZ electrolyte pellets or the YSZ membranes of the cells were recorded on a Scanning Electron Microscope Jeol JSM-5600, Shimadzu SS-550 (Japan) or Jeol JSM-6700F Field Emission Scanning Electron Microscope.

Results

The hybrid direct carbon fuel cell (HDCFC) concept

The challenge that we seek to address here is to develop a structure with sufficiently high performance that is robust enough to survive in the aggressive carbonate environment of the direct carbon fuel cell. For direct carbon oxidation a liquid–solid interaction is required at the anode, carbonates, those containing lithium carbonate are well suited to this task.[47–51] It is worth noting that a significant volume of carbonate is required, and unlike in a MCFC the carbonate cannot be retained in a supporting matrix. Yttria zirconia is the most widely utilised electrolyte in SOFC technology and offers good oxide conductivity in both oxidising and reducing environments from 700–1000 °C; however, the possibility to form lithium zirconate on reaction with molten lithium carbonate may be an issue in the fabrication of thin membranes with low resistance.

The model HDCFC shown in Fig. 1 was utilised to investigate various system configurations and geometries. In this system, carbon is oxidised in an alumina chamber, which is sealed to an SOFC type cell. The atmosphere can be controlled by flowing various gases, mainly CO_2 or N_2. A lithium–potassium carbonate eutectic with a melting temperature of 500 °C is used as the secondary electrolyte/anolyte. Oxygen ions come through the YSZ electrolyte from the cathode through molecular O_2 reduction at *e.g.* lanthanum doped strontium manganite. The model carbon fuel used in these studies is 1.6 g of pyrolysed (400 °C) medium density fibreboard (PMDF) of composition C (70.4%), N (4.6%) and H (3.5%) with the residual (21.5%) anticipated to be O as the ash content was <0.1%.

HDCFC polarisation behaviour

The significant improvement in polarisation behaviour on the sequential introduction of carbonate, decreasing of zirconia electrolyte thickness and improvement of cathode electrocatalytic behaviour is well illustrated in Fig. 2. Initially, a relatively thick electrolyte of 1 mm thickness, 20 mm diameter formed by dry pressing and sintering with a cathode of

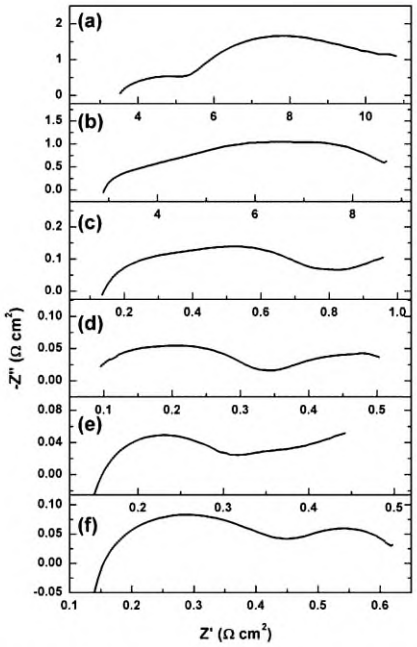

Fig. 2 Ac impedance spectra at 750 °C tested on different cells in N_2 atmosphere except for (d). (a) In the absence of carbonate with a 1 mm thick electrolyte, both of the series resistance and polarisation resistance are large; (b) in the presence of carbonate with a thick electrolyte, the series resistance of the cell is smaller in comparison to the one without carbonate; (c) using a thin electrolyte with a LSM cathode and N_2 as the purge gas, a small series resistance was obtained due to only slight ohmic loss from the electrolyte; (d) using a thin electrolyte with a LSM cathode and CO_2 as the anode purge gas improved polarization resistance is observed; (e) using thin electrolyte with a cathode of LSC in static air, the cell performance was further improved because of the good conductivity and catalytic property of the LSC cathode; (f) using a thin electrolyte with a cathode of LSC under flowing air, the cell performance was further improved because of faster gas diffusion at the cathode.

lanthanum doped strontium manganite ($(La_{0.8}Sr_{0.2})_{0.95}MnO_{3-\delta}$, LSM) and YSZ composite in a 50 : 50 weight ratio, and an anode of 60 wt% nickel oxide and 40 wt% YSZ composite applied by screen printing were assembled into a fuel cell to investigate the electrochemical performance. In the absence of carbonate slurry the total cell resistance at 750 °C was around 11 Ω cm² (Fig. 2a), which reduces to 8.7 Ω cm² (Fig. 2b) with the carbonate slurry.

The maximum power density of 70 mW cm^{-2} was obtained at 750 °C on this cell (Fig. S1†) with carbonate. The cell resistance consists of two parts, Fig. 2, one is the ohmic resistance, most of which is from the electrolyte, the electrode and the contact resistance; however, if the nickel is not fully reduced the poor lateral conductivity also impacts the ohmic resistance. The other part is the electrode reaction resistance, also called polarisation resistance which may include some concentration resistance. Fig. 2b shows 2.89 Ω cm² of series resistance, making up 33% of the total resistance of 8.7 Ω cm². On changing cell geometry to "anode"-supported from electrolyte-supported, both the ohmic resistance and the electrode reaction resistance decrease, and the total cell resistances are less than 1 Ω cm² in N_2, Fig. 2c, and 0.6 Ω cm² in CO_2, Fig. 2d. The polarisation resistance of the LSM cathode is 0.36 Ω cm² (Fig. S2†) at the testing temperature of 750 °C from symmetric cell measurement and hence contributes

70% of the total resistance of the hybrid direct carbon fuel cell (0.5 Ω cm^2). In order to further improve cell performance, lanthanum doped strontium cobalt ($La_{0.6}Sr_{0.4}CoO_{3-\delta}$) which has much lower polarisation resistance at the same temperature (0.01 Ω cm^2, Fig. S2†) is used for the cathode with a gadolinium doped ceria (CGO) interlayer to prevent from the reaction between $La_{0.6}Sr_{0.4}CoO_{3-\delta}$ (LSC) and YSZ. The cathode polarisation resistance is significantly decreased by replacing LSM (Fig. 2c) with LSC (Fig. 2e). Under flowing air, the first polarisation arc is larger, although the overall polarisation resistance is smaller than static air, Fig. 2f.

HDCFC output

Carbonate is important in the catalytic reaction since in the absence of carbonate the open circuit voltage of the HDCFC is quite low, 0.7 V, even when well-sealed.[52] Cell testing showed similar improvements as the cell structure was modified. The cell performance improved significantly, increasing from 70 to 390 mW cm^{-2} at 750 °C under a purge gas of nitrogen, when the cell configuration changed from a 1 mm thick electrolyte-supported structure to an anode-supported structure with a 5 μm thick YSZ electrolyte, Fig. 3a. Under CO_2 purge gas, the power density of the cell reached 500 mW cm^{-2} at 750 °C (Fig. 3a). By the utilisation of LSC cathode the maximum power density of 680 mW cm^{-2} at 750 °C was obtained with static air at the cathode (Fig. 3a). Under flowing air, the peak power density reached 878 mW cm^{-2}. The significant improvement of the HDCFC from 70 to 878 mW cm^{-2} is thought to result from the following factors: lower ohmic resistance and polarisation resistance, less carbonate blocking gas/liquid/solid interfaces, faster gas diffusion and transportation, highly catalytic cathode materials, flowing gas at the cathode, *etc.* A slightly higher OCV was observed under N_2, probably due to changes in the overall gas equilibria;[51] however performance under CO_2 was slightly higher than in N_2, probably related to an enhanced electrochemical process or carbonate stability. The open circuit voltage at 750 °C under CO_2 is 1.013 V, which is close to the theoretical value if the reaction is CO being oxidised into CO_2. The open circuit voltage of the HDCFC in nitrogen is 1.08 V, higher than the theoretical value of 1.03 V assuming the total reaction of the cell is eqn (1). This may be related to the complex reactions that may happen at the anode but there may also be some H_2O from the mixture of carbon and carbonate and of course there is also some other species in the fuel such as H or N.

HDCFC stability

Stability is one of the most important issues in developing new power generation technologies. A concern relating to the present hybrid concept is the stability of zirconia in contact with molten carbonate. In this study, the short-term stability in small cells without continuous fuel feed has been investigated.

Running cells at 700 mV *vs.* air, operational periods in the range 13–15 hours are typically achieved, Fig. 4. Currents generally drop from 600 mA cm^{-2} to 200–300 mA cm^{-2} in the first 1–2 hours but then remain stable for 12–14 hours before becoming unstable, *e.g.* Fig. 4a. During the initial stages, there is some hydrogen and methane, which could contribute to the power output. We consider that the availability of fuel near the electrode/zirconia interface is the limiting factor as agitation has been observed returning to the stable current level, Fig. S3†. In the experiment shown in Fig. 4 the residue that was retrieved after the experiment when current had become unstable was about 0.02 g, suggesting that the carbon had been utilised and that the initial carbonates had decomposed to the parent oxides. The amount of carbon produced as carbon oxides also

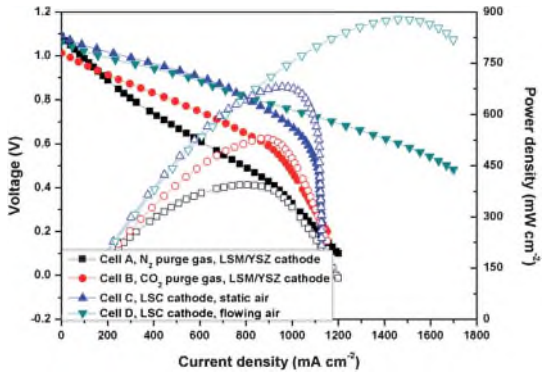

Fig. 3 Cell performance plot of the hybrid direct carbon fuel cell. Cells are based upon a nickel cermet support and a thin YSZ electrolyte with ~5 μm thickness. Having a cathode of composite of LSM/YSZ, Cell A and Cell B use N_2 or CO_2 purge gas at a flow rate of 20 ml min^{-1} in the anode, respectively; Cell C and Cell D have a LSC cathode with a $Ce_{0.9}Gd_{0.1}O_{2-\delta}$ interlayer between the cathode and the YSZ electrolyte, and the cathode is exposed to static air or 200 ml min^{-1} flowing air for Cell C and Cell D, and the flow rate of the purge gas N_2 at the anode is 20 ml min^{-1} or ~7 ml min^{-1} for Cell C and Cell D, respectively; a 2 g mixture of pyrolysed medium density fibreboard (PMDF) and Li_2CO_3–K_2CO_3 (62 : 38 mol) is supplied to the anode and all electrochemical measurements are carried out at 750 °C.

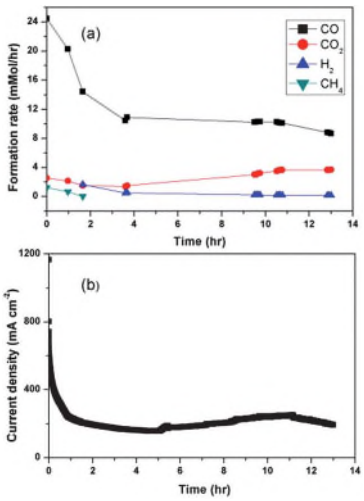

Fig. 4 Stability test of the hybrid direct carbon fuel cell under 0.7 V potential tested at 750 °C. The cell is supplied with a 2 g mixture of pyrolysed medium density fibreboard (PMDF) and Li_2CO_3–K_2CO_3 (62 : 38 mol); the cell is composed of NiO–YSZ support/5 μm YSZ thin film/CGO interlayer/LSC cathode. (a) Gas production evolution with time, measured by on-line gas chromatography; and (b) current evolution with time.

corresponded within experimental detection limits to the initial amount of carbon, Table 1. 3.2 A h (0.12 F) were passed which would correspond to 30 mmol CO_2 or 60 mmol CO produced electrochemically. The amount of gas produced was estimated to be 116 mmol CO and 26 mmol CO_2. This would correspond to 21.5% electrochemical conversion of the initial carbon to carbon dioxide if all the electrons were used in this process. The contribution from initial carbonate seems insignificant, suggesting that its role is catalytic with carbonates, oxide and CO_2 in equilibrium throughout the fuel cell test. Clearly a significant amount of carbon is pyrolysed without electrochemical conversion. As can be seen in Fig. 4b, there is a large initial rate of CO production, suggesting that pyrolysis of the MDF without electrochemical conversion occurs, probably from surface species or tars. The extent of this process relates to the large thickness of the carbon/carbonate electrode utilised in this button cell geometry. The upper surface of the electrode is some 3 cm from the electrode/electrolyte interface. This also means that produced CO_2 may undergo reverse Boudouard reaction before the CO_2 is able to escape. Despite these factors, it is worth noting that the amount of CO_2 detected is about 85%

Table 1 Carbon audit relating to the long term test shown in Fig. 4. Experiment performed for 13 hours passing 3.2 A h at 700 mV

Initial %C			% CO_x in outlet	
Carbon	Carbonate	Carbon remaining	CO	CO_2
97	3	~0%	83	17

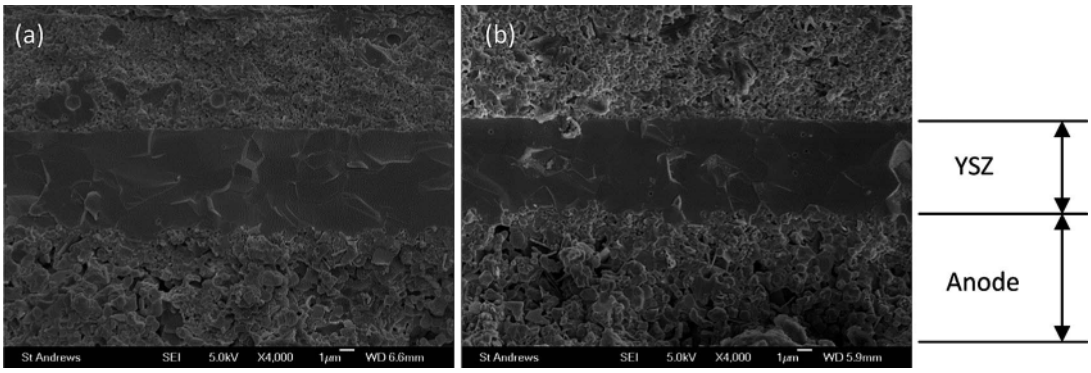

Fig. 5 Microstructure of the cells. (a) After being tested in 97%–3% H_2O and (b) after 13 hour stability test in a mixture of PMDF–carbonate under the condition shown in Fig. 4.

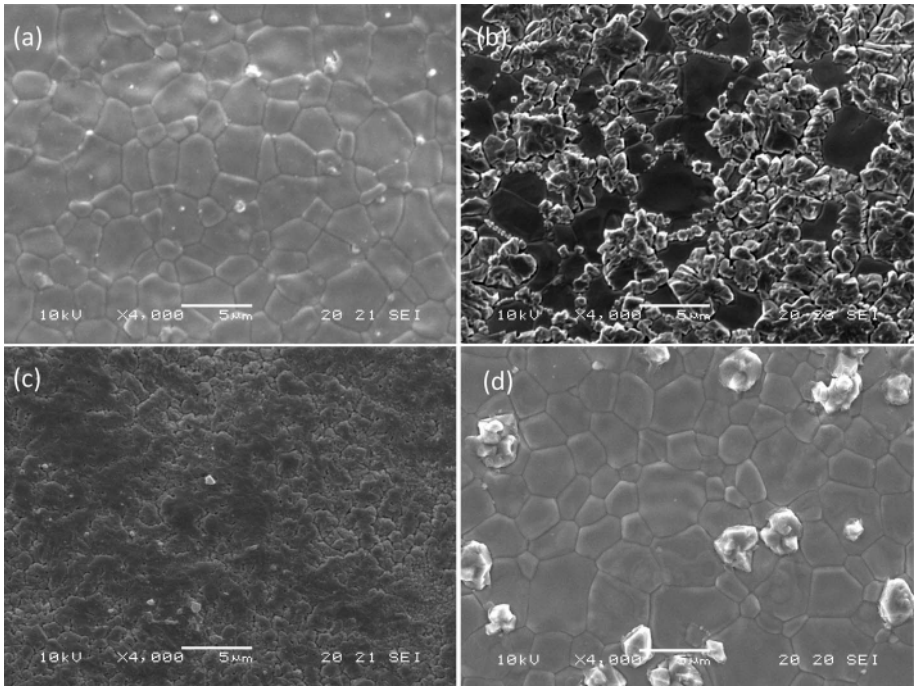

Fig. 6 YSZ membrane surface images taken after various corrosion tests were performed on pieces from previously electrochemically tested HDCFC. (a) Before corrosion test; (b) etched in lithium–potassium carbonate in air at 700 °C for 10 h; (c) etched in lithium–potassium carbonate in argon at 700 °C for 10 h; (d) etched in lithium–potassium carbonate in 5% H_2/Ar at 700 °C for 10 h.

of that that would be produced if all the electrons were produced from carbon oxidation. Increasing flow rate of the purge gas or increasing temperature above 750 °C are both observed to decrease the amount of CO_2 produced, favouring CO.

YSZ stability

A particularly surprising aspect is the apparent stability of YSZ membranes 5–10 μm thick in contact with the molten carbonate anolyte, with no significant change to the YSZ electrolyte without contact with molten carbonate (Fig. 5a) and after 13 h testing (Fig. 5b). In Fig. S4†, the cross-section of another cell shows the YSZ electrolyte membrane with 5 μm thickness after running for 2.5 h in CO_2 under fuel cell test at >200 mA cm^{-2} and this also shows good chemical resistance to the carbonate under load.

Previous experience has indicated that lithium zirconate can form on contact between this molten carbonate and yttria zirconia with catastrophic membrane failure, so we have investigated this in more detail. Fig. 6a shows the YSZ surface of a portion from a cell that had undergone electrochemical testing over 6 hours and this YSZ shows no evidence of surface change. Corrosion tests carried out in air at high temperature show marked surface corrosion, Fig. 6b. Performing the same corrosion test on the YSZ electrolyte in an inert atmosphere (argon) also showed evidence of corrosion but significantly less, Fig. 6c. Performing the same test under flowing 5% H_2 shows no evidence of corrosion in the eutectic molten carbonate, Fig. 6d. Thus it seems that the eutectic molten carbonate seems only to damage the YSZ electrolyte in oxidising atmosphere/conditions. Further evidence of etching and reorganisation of YSZ pellet surfaces is seen in Fig. S5b†, comparing the unaged YSZ surface in Fig. S5a†. The YSZ electrolyte in inert (argon) and especially in reducing atmosphere in Fig. S5c and d†, respectively, shows good chemical resistance to the eutectic molten carbonate. This is understandable as oxidising power and basicity are correlated through the Lux-Flood basicity model, as under oxidising conditions peroxide and superoxide species are likely to form, but not under reducing conditions. Under the operation of the HDCFC, the anode chamber was in reducing conditions and the YSZ electrolyte showed apparent stability.

Conclusion

We have developed a hybrid direct carbon fuel cell with a solid oxide ion conductor as the electrolyte, which separates solid carbon fuel distributed in the carbonate in the anode from oxygen oxidant in the cathode. The cell configuration with a thin YSZ electrolyte is able to resist carbonate corrosion due to it being under reducing conditions and at the same time enhancing the cell performance with the carbonate. The present lab-scale system demonstrated the feasibility of solid carbon direct conversion with high current densities.

Acknowledgements

We thank EPSRC and Carbon Trust for financial support and Robert Marshall for providing PMDF.

References

1 *Direct Carbon Fuel Cells: Converting Waste to Electricity*, R. H. Rolk, S. Lux, S. Gelber, F. H. Holcomb, ERDC-CERL Fuel Cell Program, 2007.
2 G. A. Hackett, J. W. Zondlo and R. Svensson, *J. Power Sources*, 2007, **168**, 111–118.
3 S. Yoshida, J. Matsunami, Y. Hosokawa, O. Yokota, Y. Tamaura and M. Kitamura, *Energy Fuels*, 1999, **13**, 961–964.
4 X. Li, Z. H. Zhu, R. De Marco, J. Bradley and A. Dicks, *J. Power Sources*, 2010, **195**, 4051–4058.
5 M. Ihara and S. Hasegawa, *J. Electrochem. Soc.*, 2006, **153**, A1544–A1546.
6 S. Hasegawa and M. Iharaz, *J. Electrochem. Soc.*, 2008, **155**, B58–B63.
7 M. Ihara, K. Matsuda, H. Sato and C. Yokoyama, *Solid State Ionics*, 2004, **175**, 51–54.
8 H. Saito, S. Hasegawa and M. Ihara, *J. Electrochem. Soc.*, 2008, **155**, B443–B447.
9 E. L. K. Mui, D. C. K. Ko and G. Mckay, *Carbon*, 2004, **42**, 2789–2805.
10 M. J. Antal and G. C. Nihous, *Ind. Eng. Chem. Res.*, 2008, **47**, 2442–2448.
11 T. Nunoura, K. Dowaki, C. Fushimi, S. Allen, E. Meszaros and M. J. Antal, *Ind. Eng. Chem. Res.*, 2007, **46**, 734–744.
12 S. L. Jain, J. B. Lakeman, K. D. Pointon and J. T. S. Irvine, *J. Fuel Cell Sci. Technol.*, 2007, **4**, 280–282.
13 S. L. Jain, J. B. Lakeman, K. D. Pointon and J. T. S. Irvine, in *Solid Oxide Fuel Cells 10*, ed. K. Eguchi, S. C. Singhai, H. Yokokawa and H. Mizusaki, 2007, vol. 7, pp. 829–836.
14 S. Zecevic, E. M. Patton and P. Parharni, *Carbon*, 2004, **42**, 1983–1993.
15 W. W. Jacques, *US. Pat.*, 555111, 1896.
16 W. W. Jacques, *Haper's Magazine*, 1896–1897, **94**, 144.
17 M. Anbar, D. F. McMillen, R. D. Weaver, P. J. Jorgensen and A. Weaver, *US. Pat.*, 3970474, 1976.
18 T. T. Tao, W. Bai, S. Rackey and G. Wang, *PCT. Pat.*, Applicant No. PCT/US2002/020099, 2003.
19 A. Jayakumar, R. Kungas, S. Roy, A. Javadekar, D. J. Buttrey, J. M. Vohs and R. J. Gorte, *Energy Environ. Sci.*, 2011, **4**, 4133–4137.
20 J. F. Copper, N. Cherepy and R. L. Krueger, *US. Pat.*, 6815105, 2004.
21 J. F. Copper, N. Cherepy and R. L. Krueger, *US. Pat.*, 6878479, 2005.
22 N. J. Cherepy, R. Krueger, K. J. Fiet, A. F. Jankowski and J. F. Cooper, *J. Electrochem. Soc.*, 2005, **152**, A80–A87.
23 S. Li, A. C. Lee, R. E. Mitchell and T. M. Gur, *Solid State Ionics*, 2008, **179**, 1549–1552.
24 Y. Nabae, K. D. Pointon and J. T. S. Irvine, *J. Electrochem. Soc.*, 2009, **156**, B716–B720.
25 L. J. Jia, Y. Tian, Q. H. Liu, C. Xia, J. S. Yu, Z. M. Wang, Y. C. Zhao and Y. D. Li, *J. Power Sources*, 2010, **195**, 5581–5586.
26 S. Nurnberger, R. Bussar, P. Desclaux, B. Franke, M. Rzepka and U. Stimming, *Energy Environ. Sci.*, 2010, **3**, 150–153.
27 W. H. A. Peelen, K. Hemmes and J. H. W. de Wit, *Proc. European Research Conference on Molten Salts*, Poquerolles, France, June 27-July3, 1998.
28 J. B. Lakeman, K. D. Pointon, J. T. S. Irvine and J. Badley, *Distillation*, 2004, **07**, 401–407.
29 K. Pointon, B. Lakeman, J. Irvine, J. Bradley and S. Jain, *J. Power Sources*, 2006, **162**, 750–756.
30 A. S. Lipilin, I. I. Balachov, L. H. Dubois, A. Sanjurjo, M. C. Mckubre, S. Crouch-Baker, M. D. Hornbostel and F. L. Tanzclla, *US. Pat.*, Application No. PCT/US2005/017963, 2005.
31 I. I. Balachov, L. H. Dubois, M. D. Hornbostel and A. S. Lipilin, *Direct Carbon Fuel CellWorkshop*, Palm Springs, CA, USA, 14th November, 2005.
32 Y. G. Pan, E. Velo, X. Roca, J. J. Manya and L. Puigjaner, *Fuel*, 2000, **79**, 1317–1326.
33 A. C. Lee, S. Li, R. E. Mitchell and T. M. Guer, *Electrochem. Solid-State Lett.*, 2008, **11**, B20–B23.
34 X. Li, Z. H. Zhu, R. De Marco, A. Dicks, J. Bradley, S. M. Liu and G. Q. Lu, *Ind. Eng. Chem. Res.*, 2008, **47**, 9670–9677.
35 D. G. Vutetakis, D. R. Skidmore and H. J. Byker, *J. Electrochem. Soc.*, 1987, **134**, 3027–3035.
36 C. Li, Y. X. Shi and N. S. Cai, *J. Power Sources*, 2010, **195**, 4660–4666.
37 T. M. Gur, M. Homel and A. V. Virkar, *J. Power Sources*, 2010, **195**, 1085–1090.

38 Y. Bai, Y. Liu, Y. Tang, Y. Xie and J. Liu, *Int. J. Hydrogen Energy*, 2011, **36**, 9189–9194.
39 A. C. Lee, R. E. Mitchell and T. M. Gur, *J. Power Sources*, 2009, **194**, 774–785.
40 A. C. Lee, R. E. Mitchell and T. M. Gur, *AIChE J.*, 2009, **55**, 983–992.
41 C. Xia, L. Li, Y. Tian, Q. H. Liu, Y. C. Zhao, L. J. Jia and Y. D. Li, *J. Power Sources*, 2009, **188**, 156–162.
42 J. B. Huang, L. Z. Yang, R. F. Gao, Z. Q. Mao and C. Wang, *Electrochem. Commun.*, 2006, **8**, 785–789.
43 T. M. Gur, *J. Electrochem. Soc.*, 2010, **157**, B751–B759.
44 Y. Z. Wu, C. Su, C. M. Zhang, R. Ran and Z. P. Shao, *Electrochem. Commun.*, 2009, **11**, 1265–1268.
45 M. Homel, T. M. Gur, J. H. Koh and A. V. Virkar, *J. Power Sources*, 2010, **195**, 6367–6372.
46 X. Y. Zhao, Q. Yao, S. Q. Li and N. S. Cai, *J. Power Sources*, 2008, **185**, 104–111.
47 D. X. Cao, G. L. Wang, C. Q. Wang, J. Wang and T. H. Lu, *Int. J. Hydrogen Energy*, 2010, **35**, 1778–1782.
48 M. M. Chen, C. Y. Wang, X. M. Niu, S. Zhao, J. Tang and B. Zhu, *Int. J. Hydrogen Energy*, 2010, **35**, 2732–2736.
49 S. L. Jain, J. B. Lakeman, K. D. Pointon, R. Marshall and J. T. S. Irvine, *Energy Environ. Sci.*, 2009, **2**, 687–693.
50 S. L. Jain, Y. Nabae, B. J. Lakeman, K. D. Pointon and J. T. S. Irvine, *Solid State Ionics*, 2008, **179**, 1417–1421.
51 Y. Nabae, K. D. Pointon and J. T. S. Irvine, *Energy Environ. Sci.*, 2008, **1**, 148–155.
52 C. R. Jiang and J. T. S. Irvine, *J. Power Sources*, 2011, **196**, 7318–7322.